Boundary-Layer Meteorol (2006) 121:351–375
DOI 10.1007/s10546-006-9074-4

RESEARCH ARTICLE

Methodological considerations regarding the measurement of turbulent fluxes in the urban roughness sublayer: the role of scintillometery

Matthias Roth · Jennifer A. Salmond · A. N. V. Satyanarayana

Received: 17 November 2005 / Accepted: 20 March 2006 /
Published online: 3 June 2006

Abstract We address some of the methodological challenges associated with the measurement of turbulence and use of scintillometers in the urban roughness sublayer (RSL). Two small-aperture scintillometers were located near the roof interface in a densely urbanized part of Basel, Switzerland, as part of the Basel Urban Boundary-Layer Experiment (BUBBLE) in the summer of 2002. Eddy correlation instruments were co-located near the mid-point of each scintillometer path for data verification purposes. The study presents the first values of the inner length scale of turbulence (l_0) and the refractive index structure parameter of air (C_n^2) for a city and demonstrates the influence of mechanical driven turbulence on dissipation. Comparison of dissipation values determined from the two approaches show large scatter that is possibly due to the spatial inhomogeneity of the turbulence statistics within the RSL. Velocity and temperature spectra display a $-2/3$ slope in the inertial subrange, although the spectral ratio is less than the theoretical prediction of 4/3 expected for isotropy. Conventional Monin–Obukhov equations used to calculate fluxes from the scintillometer were replaced with urban forms of the equations. The results suggest that the scintillometer may be an appropriate tool for the measurement of sensible heat flux (Q_H) above the rooftops given a suitable determination of the effective measurement height.

Keywords Monin–Obukhov similarity · Roughness sublayer · Scintillometer · Urban turbulence · Zero-plane displacement length

M. Roth (✉)· A. N. V. Satyanarayana
Department of Geography, National University of Singapore, 1 Arts Link, Kent Ridge, Singapore 117570
e-mail: geomr@nus.edu.sg

J. A. Salmond
Division of Environmental Health and Risk Management, School of Geography, Earth and Environmental Sciences, University of Birmingham, Birmingham, UK

1 Introduction

The spatial heterogeneity of urban surfaces presents a particular challenge to the measurement of turbulent fluxes, and is particularly true in the roughness sublayer (RSL) close to the urban surface. Here the mosaic of rooftop and street canyon surfaces presents a complex three-dimensional source area resulting in microscale flux fields within and just above the urban canopy that are highly variable in space and time, with flow fields that are influenced by the direct interaction with roughness elements. Effects include local pressure gradients related to form drag on the obstacles and wake production. In the upper part of the RSL above a height that is determined by the height and spacing of the buildings (e.g. Roth 2000), the horizontal variability disappears (in the time average) and a "constant" flux layer (surface layer) is present where standard micrometeorological theory has been shown to apply. Because of these complexities, most studies try to avoid this region and little is known about the characteristics of turbulent fluxes within the RSL, nor the relative importance of rooftop versus street canyon surfaces in determining the overall characteristics of the urban boundary layer. This has consequences not only for our understanding of the processes driving the urban boundary layer but also for our ability to model pollutant dispersion pathways.

Scintillometery provides an alternative approach to obtaining more spatially representative datasets in the RSL. Scintillometers provide a measurement of the refractive index structure parameter of air (C_n^2), and in the case of bichromatic instruments an additional measurement of the inner length scale of turbulence (l_0), integrated along an optical path. Using standard Monin–Obukhov similarity (MOS) theory variations in these variables can be used to calculate turbulent fluxes (e.g. Thiermann and Grassl 1992; Hill et al. 1992). The optimal path length varies according to the aperture size of the scintillometer. For example a large-aperture scintillometer can be used over distances of a few kilometres whilst a small-aperture scintillometer is typically used over distances of less than 200 m. Thus scintillometery offers the ability to make path-averaged measurements of turbulent fluxes of heat and momentum, which can be a considerable advantage in areas where the source area is non-homogeneous.

The averaging times needed for flux calculations from a scintillometer are also thought to be shorter compared to those based on standard eddy correlation (EC) instruments, as a result of the increased spatial sampling of turbulent eddies (De Bruin et al. 2002). This is particularly advantageous in heterogeneous environments where the theoretical constraints of stationarity may not be met for prolonged periods of time. Such time-averaging benefits, however, have recently been questioned by Andreas et al. (2003) who conclude that turbulent fluxes inferred from non-stationary scintillometer statistics can also be uncertain.

Scintillometers have been shown to be effective instruments for the measurement of line-averaged turbulent fluxes of heat and momentum under conditions where the usual restrictions for the applicability of MOS apply, i.e. at sufficient heights over homogeneous, low-roughness surfaces. Examples of the successful application of small-aperture scintillometers (same type of sensor as used in the present study) include Kohsiek (1982), Hill et al. (1992), Thiermann and Grassl (1992), Hill (1997), Green et al. (1994), De Bruin et al. (2002) and Hartogensis et al. (2002).

The validity of the assumptions underlying the calculation of turbulent fluxes using parameters measured by the scintillometer, however, may be problematic in the urban atmosphere. MOS cannot be directly applied close to the urban surface where the flow

is non-stationary and the turbulence properties vary in space (Rotach 1993a; Roth 1993, 2000; Roth and Oke 1993). Further, the calculated fluxes rely on accurate measurements of height above the surface. For the near-rooftop interface estimation of this height becomes problematic and Grimmond and Oke (1999) clearly demonstrate the difficulties associated with all currently used approaches to assigning an effective measurement height to the urban surface.

It is therefore not surprising that only very few applications of scintillometery in the urban atmosphere are available despite the potential benefits of this method. Possibly the first measurements were carried out over a densely built-up shopping district of Tokyo (Kanda et al. 1997); this exploratory work was followed by observations over a densely built-up residential neighbourhood of Tokyo (Kanda et al. 2002). Two small-aperture scintillometers were installed at normalized heights $z/z_H = 3.8$ and 1.9, respectively (where z is measurement height above surface and z_H is the average height of buildings). Ideally, sensors for turbulent flux measurements should be carried out above the top of the RSL, i.e. within the constant flux layer if one exists, which can be found at $z/z_H > 2$–3 (e.g. Roth 2000). The upper measurement level in the Tokyo experiment is therefore within the constant flux layer, whereas the lower level is probably located near its lower boundary. Using modified forms of MOS equations (evaluated locally rather than using the 'rural' ones provided by the scintillometer software) sensible heat fluxes (Q_H) obtained by the scintillometer at the top level for a few hours on 2 days agreed well with 30-min averages from a separate EC system located at the same height and location (scintillometer values were slightly larger but differences were $< 10\%$ for most values). The second scintillometer at the lower height was used to test the applicability of a new method to estimate the zero-plane displacement length (z_d) that uses simultaneous scintillometer measurements of Q_H at two different heights (Kanda et al. 2002).

Large-aperture scintillometers (LAS) were employed during 1 month in summer of 2001 as part of the ESCOMPTE project in Marseille (Lagouarde et al. 2006; Mestayer et al. 2005). Multiple sensors were installed over the city centre of Marseille along three different paths of approximately 2 km length, 26–53 m ($z/z_H = 1.5$–5) above the uneven surface consisting of old buildings and narrow streets. Output values were sampled at 1 Hz and averaged over 15 min. Sensible heat fluxes were determined by combining the LAS-derived surface-layer temperature scale (T_*) with an independently determined friction velocity (u_*) from a co-located EC system and directly from the LAS-derived temperature structure parameter (C_T^2) assuming free convection, respectively. Q_H measured by the two methods agreed well with each other for unstable conditions with a slight systematic underestimation of the latter. Comparison with independent values from EC measurements at $z/z_H = 2.8$ along one of the paths was also very good with the exception of a few occasions when the LAS values were below (above) the daytime peak (nighttime) EC values. The scintillation spectra of the urban refractive index fluctuations were also investigated by Irvine et al. (2002).

In the present study we address some of the measurement and methodological issues associated with the use of scintillometers in the urban RSL. The past urban applications referred to earlier have all been made in the upper part of the RSL or higher. Further, they only report Q_H although 50 v small-aperture scintillometers measure u_* as well. Often, however, operational limitations do not allow observations to be carried out at sufficient heights that avoid the RSL, and the momentum flux is a fundamental atmospheric property needed in a wide range of applications. Scintillometery relies on MOS theory, which, however, is violated close to an inhomogeneous

surface and theoretically makes this approach invalid in the RSL. On the other hand a number of urban studies have shown that MOS can still be used in the RSL with modified empirical constants (e.g. Rotach 1993b; Roth 1993; Roth and Oke 1993; Feigenwinter et al. 1999). It is therefore worthwhile trying to evaluate the feasibility of this approach in the RSL because it offers a range of potential advantages as mentioned above. The observations for this study were made very close to the urban surface located in an area of extreme flow heterogeneity across the top of a street canyon and along the adjacent rooftops. These two facets are the dominant components of the urban surface. Modified forms of the MOS equations are obtained from EC data and used to calculate the scintillometer quantities Q_H and u_*. The zero-plane displacement length (z_d) and effective measurement height ($z' = z - z_d$) are estimated using various morphometric approaches based on fetch and source area considerations.

2 Theoretical background

The particular bichromatic, small-aperture scintillometer used in the present study (Scintec SLS20, referred to as SLS from here onwards) measures l_0 and C_n^2 from which the dissipation for turbulent kinetic energy (TKE), ε, and temperature structure parameter, C_T^2, can be directly determined. Here, l_0 is linked to ε through

$$\varepsilon = \nu^3 \left(\frac{7.4}{l_0}\right)^4, \tag{1}$$

where ν is the kinematic viscosity of air. C_T^2 can be written as

$$C_T^2 = C_n^2 \left(\frac{T^2}{p\gamma}\right)^2, \tag{2}$$

where p is the air pressure, T is the air temperature and γ is a constant. Equation (2) ignores the humidity contributions, which, however, are small in the urban environment where the Bowen ratio is typically much larger than unity.

The non-dimensional forms for ε and C_T^2 are given by

$$\phi_\varepsilon = \frac{kz'\varepsilon}{u_*^3}, \tag{3}$$

$$\phi_{CT} = \frac{C_T^2 (kz')^{2/3}}{T_*^2}, \tag{4}$$

where k is the von Karman constant (here taken as 0.4). C_T^2 can be related to the dissipation rate of heat, N^* and ε by (Corrsin 1951)

$$C_T^2 = 4\beta_1 N^* \varepsilon^{-1/3}, \tag{5}$$

where $\beta_1 = 0.86$ (Obukhov–Corrsin constant), which can be transformed into a non-dimensional form (Thiermann and Grassl 1992)

$$\phi_{CT} = 4\beta_1 \phi_N \phi_\varepsilon^{-1/3} \tag{6}$$

with

$$\phi_N = \frac{N^* k z'}{u_* T_*^2}. \tag{7}$$

Here, u_* and T_* are calculated using an iterative solution to the following equations:

$$u_*^2 = v^2 \left(\frac{7.4}{l_0}\right)^{8/3} k z'^{2/3} \phi_\varepsilon^{-2/3}(\zeta), \tag{8}$$

$$T_*^2 = C_T^2 \left(k z'\right)^{2/3} \phi_{CT}^{-1}(\zeta), \tag{9}$$

$$L_v = \frac{T_v u_*^2}{k g T_*}, \tag{10}$$

where L_v is the Obukhov length, $\zeta = z'/L_v$, T_v is the virtual temperature and g is the acceleration due to gravity.

The momentum and sensible heat fluxes follow from

$$\tau = -\rho u_*^2, \tag{11}$$

$$Q_H = -\rho c_p u_* T_*, \tag{12}$$

where ρ is density of air and c_p is specific heat of air.

ϕ_ε and ϕ_{CT} are calculated using MOS theory. The software provided with the SLS uses the following forms of the MOS equations for unstable conditions (Thiermann and Grassl 1992):

$$\phi_\varepsilon(\zeta) = (1 - 3\zeta)^{-1} - \zeta, \quad (\zeta < 0) \tag{13}$$

$$\phi_{CT}(\zeta) = 4\beta_1 \left[1 - 7\zeta + 75(\zeta)^2\right]^{-1/3}. \quad (\zeta < 0) \tag{14}$$

Equations (13) and (14) differ slightly from the corresponding similarity equations proposed by Wyngaard et al. (1971) and Wyngaard (1973) and employed in studies by e.g. Green et al. (1994) and Andreas et al. (2003) of the form (assuming $k = 0.35$):

$$\phi_\varepsilon(\zeta) = \left(1 + 0.5|\zeta|^{2/3}\right)^{3/2}, \quad (-2 \le \zeta \le 0) \tag{15}$$

$$\phi_{CT}(\zeta) = 4.9(1 + 7|\zeta|)^{-2/3}. \quad (\zeta < 0) \tag{16}$$

Equations (13) and (14) are also preferred by Hill (1997) using supporting evidence from Frenzen and Vogel (1992) and Vogel and Frenzen (1992) for the lower ϕ_ε values observed closer to neutral stability that are not captured by Equation (15). Given the differences associated with these homogeneous surface-layer forms and the fact that a priori there is no reason why MOS should apply in the urban atmosphere close to the buildings [where parameters such as building height may influence the structure of turbulence and where fluxes are not constant with height], urban-specific forms of the MOS equations are calculated from EC data observed at the present site (Section 4.3). These newly developed urban forms will be compared to those obtained by EC techniques and employed in the scintillometery work of Kanda et al. (2002) using suburban dissipation data from Tokyo and Vancouver, Canada,

$$\phi_\varepsilon(\zeta) = (1 - 10.5\zeta)^{-1} - \zeta, \qquad (-3 < \zeta < 0) \quad (17)$$

$$\phi_N(\zeta) = 0.68\,(1 - 9.69\zeta)^{-1/2}, \qquad (-3 < \zeta < 0) \quad (18)$$

$$\phi_{CT}(\zeta) = 4\beta_1 \left[0.68\,(1 - 9.69\zeta)^{-1/2}\right]\left[(1 - 10.5\zeta)^{-1} - \zeta\right]^{-1/3}. \qquad (-3 < \zeta < 0) \quad (19)$$

Dissipation values can also be calculated from the high-frequency end of spectra obtained by fast-response turbulence sensors. The following equations are based on predictions for the inertial subrange of turbulence spectra (e.g. Kaimal et al. 1972):

$$\varepsilon = \left[n\,S_{u,v,w}(n)\right]^{3/2} (2\pi n/U)\; A^{3/2}, \quad (20)$$

$$N^* = [n\,S_T(n)]\,(2\pi n/U)^{2/3}\; \varepsilon^{1/3}\, B_T^{-1}, \quad (21)$$

where n is natural frequency (in s^{-1}), S is spectral energy density, u, v, w are longitudinal, transverse and vertical velocity components, T is temperature, U is mean wind speed, A is a universal constant for the inertial subrange (0.73 for v and w and 0.55 for u) and $B_T = 0.78$ is a constant analogous to A.

As can be seen from the equations above, MOS theory is inherently reliant on the accurate specification of z_d, which depends on the size, shape, distribution and density of the roughness elements in an urban area. It can be calculated either using morphometric techniques that use measurements of surface dimensions and geometry, or micrometeorological techniques that rely on the use of field observations and the logarithmic wind profile (Grimmond and Oke 1999). Although Grimmond and Oke outline a variety of different approaches for the estimation of z_d, there is little consensus in the literature as to the most reliable technique and both approaches have limitations. For our purposes we draw upon a variety of morphometric techniques for the estimation of z_d. This is discussed further in Section 3.2.

3 Experimental

3.1 Site description and instrumentation

The experiment took place in Basel, Switzerland as part of BUBBLE (Basel Urban Boundary-Layer Experiment), which was a year-long project to investigate in detail the boundary-layer structure over a European city. Measurements of energy fluxes, turbulence statistics, boundary-layer profiles and a tracer experiment were conducted during an intensive observation period (IOP) at several sites with different urban and rural characteristics in summer 2002 (see Rotach et al. 2005 for more details). The particular site used for the present study (Basel–Sperrstrasse) is characterized by urban land-use and made up of street canyons bounded by mainly 3–4 storey residential buildings (Fig. 1). The following morphometric data for this particular site were determined from a high-resolution 3D model of the city for a circle of diameter 250 m on the site: $z_H = 14.6$ m; standard deviation of building height (σ_{zH}) = 6.9 m; plan aspect ratio (λ_p: plan area of roughness elements relative to total surface area) = 0.54; mean frontal aspect ratio (λ_f: frontal area of roughness elements 'seen' by the oncoming wind relative to total surface area) = 0.37; complete aspect ration (λ_c: total surface of roughness elements exposed to airflow relative to total surface area) = 1.92; local street canyon aspect ratio at tower base (λ_s: height to width ratio) = 1 (Rotach et al. 2005).

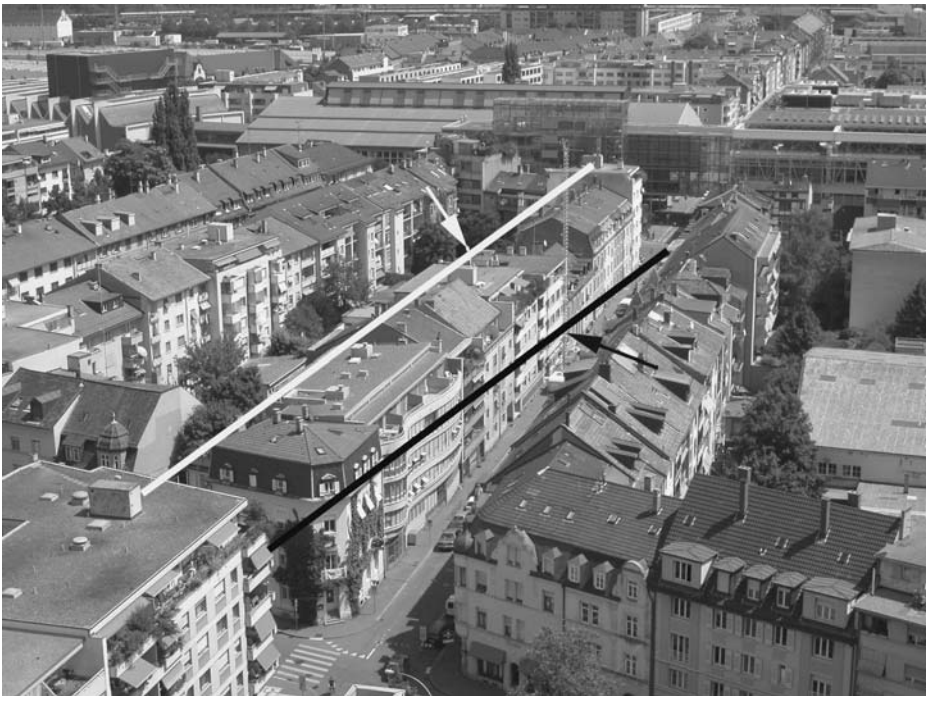

Fig. 1 Photograph showing location of scintillometer paths (white line—rooftops; black line—canyon-top) and location of sonic anemometers near the mid-point of the respective path (white arrow—rooftops; black arrow—canyon-top)

For the purpose of the present study two SLS instruments were placed in close proximity to the main instrumented tower at the Sperrstrasse site (Fig. 1). This tower was located near the mid-point of the block that was considered representative of the urban core of Basel, in an area of the city characterized by relatively uniform land use. The tower was instrumented with sonic anemometers at $z = 3.6$, 11.3, 14.7, 17.9, 22.4 and 31.7 m on booms extending towards the middle of the street canyon. A further sonic anemometer was located 11.3 m above canyon floor, 0.65 m from the north wall of the canyon. One SLS was mounted just below roof level diagonally across the Sperrstrasse street canyon at 13.5 m above street level ($z/z_H = 0.92$). The mid-point of the optical path (length = 116 m) roughly coincided with the sonic anemometer (Gill R2) mounted on the tower at $z = 14.7$ m ($z/z_H = 1.01$). The second SLS was located 19.3 m above street level ($z/z_H = 1.32$) about 3–5 m above the irregular roof height along the north side of the Sperrstrasse canyon. The mid-point of the optical path (length = 171 m) coincided with a further sonic anemometer (Campbell Scientific CSAT) located at $t = 19.3$ m (3.5 m above local roof height) on the rooftop. Due to practical considerations, the end of both the street canyon and rooftop SLS paths crossed a road intersection. However, given that the SLS turbulence functions are calculated using a weighted bell-shaped curve that places emphasis on observations made near the middle of the beam, conditions close to both the receiver and transmitter have little effect on the calculated turbulence parameters.

The sonic anemometer output was recorded at about 20 Hz and averaged over 30 min. The raw data were rotated into the mean horizontal wind and linear de-trending was performed to calculate (co)spectra, fluxes and other turbulence statistics. Density and temperature variance corrections were applied where applicable (Webb et al. 1980; Liu et al. 2001). Care was taken to exclude data from wind directions with the potential for flow interference due to the tower or other sensors mounted upwind. Cases with very low sensible heat flux densities (0–5 $W\,m^{-2}$), wind speeds (usually $< 0.1\,m\,s^{-1}$) and vertical flow angles $> |30|$ deg (necessary for canyon location only) were also excluded. The SLS calculates turbulence statistics with an averaging time of 1 min. Thirty 1-min fluxes were further averaged to provide one 30-min average that corresponds to the sonic flux-averaging period. Due to spatial averaging, 1-min SLS statistics are thought to be sufficient for the representation of fluxes (De Bruin et al. 2002) and are probably not very different from 30-min averages calculated from raw data. This is unlike fluxes measured using the standard EC approach that rely on longer averaging periods. Prior to the experiment the two scintillometers were compared at a grassland site and showed good agreement (30-min averages were within 5% of each other). Periods when the diagnostic software of the scintillometer reported less then 80% error free data in the computation of the 1-min statistics were eliminated, and were usually associated with rain events.

Data were collected during the summertime BUBBLE IOP between 26 June and 12 July 2002. During this period the mean air temperature was 20°C and rainfall (mostly from thunderstorms) was 65 mm. Winds 10 m above z_H were on average $2.0\,m\,s^{-1}$ (Christen and Vogt 2004). Figure 2 shows the distribution of wind speed and direction at the two measurement levels. The rooftop level experiences the typical distribution of wind directions at this site due to the particular thermal circulation in the Rhine valley with daytime (nighttime) winds primarily from the western through to the northern sectors (eastern through southern sectors). Canyon-top winds are generally weaker and exhibit some channelling of the flow along the canyon axis with the nighttime winds from the eastern sector.

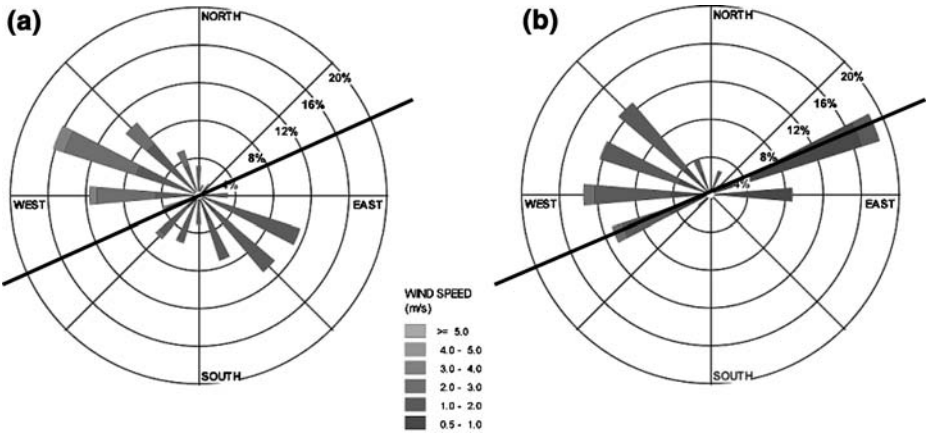

Fig. 2 Frequency distribution of wind direction and speeds of observations used in present analysis above (**a**) rooftops and (**b**) canyon. Solid line—canyon axis

Table 1 Summary of zero-plane displacement length (z_d) and effective measurement heights ($z' = z - z_d$) from a number of morphometric approaches

Study	Canyon scintillometer (EC)				Roof scintillometer and EC			
	z	z_H	z_d	z'	z^{d}	z_H^{d}	z_d	z'
Grimmond and Oke (1999)	13.5 (14.7)	14.6	11.7[a]	1.8 (3.0)	9.3	7	5.6[a]	3.7
Bottema (1995)	13.5 (14.7)	14.6	10.1[b]	3.4 (4.6)	9.3	7	4.7[c]	4.6
Raupach (1994)	13.5 (14.7)	14.6	9	4.5 (5.7)	9.3	7	4.3	5
MacDonald et al. (1998)	13.5 (14.7)	14.6	11.6	1.9 (3.1)	9.3	7	5.6	3.7
Christen et al. (2004)	13.5 (14.7)	14.6	–	5.5 (5.5)	–	–	–	–
Present study	13.5 (14.7)	14.6	10.6	3.4 (4.4)	9.3	7	5	4.3

The present value is the average of all values for the canyon-top and rooftop positions, respectively.
z — sensor height, z_H — average height of buildings
[a]coefficient = 0.8, [b]porosity = 0.5, [c]porosity = 0.8, [d]after allowing 10 m for courtyard infill (see text)

3.2 Estimates of z_d for the canyon and rooftop source areas

In surface-layer scaling, the dominant length scale is the distance above the effective surface, which in the urban case needs to take into account the existence of z_d. This scaling, however, fails in the RSL because the turbulence properties also depend on the characteristics and dimensions of the surface roughness elements and it is probable that z_d varies spatially. A further complication in the RSL is the inapplicability of aerodynamic methods to estimate z_d in a region where the logarithmic shape of the neutral wind profile is not given (Rotach 1993a). Morphometeric methods, which rely on simple surface description and do not require wind observations to estimate z_d, have been shown to be useful over a variety of rough surfaces (Grimmond and Oke 1999) and will therefore be employed in the present study.

Application of the various morphometric approaches to our sites results in a range of z_d values (Table 1). The standard 'rule of thumb' (Grimmond and Oke 1999), equates z_d to a fraction of mean z_H, and for high-density sites Grimmond and Oke suggest a coefficient of about 0.8. This value assumes skimming flow, which should be the case for the present site with a canyon height-to-width (H/W) ratio > 1. Other methods in Table 1 take into consideration the areal fraction and height of different land-use types (Bottema 1995), frontal aspect ratio (Raupach 1994) and plan aspect ratio (MacDonald et al. 1998) and produce values of similar magnitude. For the canyon-top location an additional method by Christen et al. (2004) was used. They suggest a constant z' value for any level within the canyon that is computed as half the canyon width or the radius of the largest eddy that fits into it. Their approach is supported by the fact that the peak frequencies of TKE spectra and Eulerian length scales do not vary significantly with height within the canyon (Christen et al. 2004).

The characteristics of the source area in the immediate vicinity of the rooftop sensors make the use of the morphometric approaches difficult. Using the *FSAM* source area model (Schmid 1994) as a guide, the dominant source area for the rooftop site was shown to be located within 10–200 m of the instrument. Figure 1 illustrates that this includes roof surfaces, street surfaces and the surrounding courtyards, many of which include lower height buildings. In some wind direction sectors street canyons account for as little as 3% (mean 16%) of the total land cover, whilst the courtyard buildings account for up to 50% (mean 25%) of the land area (Table 2). This suggests

Table 2 Percentage land cover within a 200-m radius of the site calculated using a simple land classification scheme with four categories (buildings, courtyard infill, tree cover and street canyon surfaces) for each of the eight wind sectors

Sector	Buildings $h = 17$ m	Courtyard infill $h = 10$ m	Trees $h = 1$–10 m	Street canyon and courtyard surfaces $h = 0$ m
1 North	50	17	13	20
2 North-east	73	9	13	5
3 East	53	17	17	13
4 South-east	38	52	7	3
5 South	33	49	10	8
6 South-west	33	30	13	23
7 West	63	17	10	10
8 North-west	53	12	6	28
Mean (%)	50	25	9	16

h—height

that the reference surface for the calculation of z_d for the 17 m buildings under the SLS path is not dominated by street level surfaces but by surfaces 10 m above ground at the height of the courtyard buildings and treetops. The actual sensor and building heights were therefore reduced by 10 m.

Because no one approach can be expected to yield the "correct" z_d and hence z' value, the average from the various approaches was used in the calculations. The range of values is reasonably small at the rooftop level but larger at canyon-top (Table 1). Considering the differences in the approaches used, some variability can be expected and, given the sensitivity of the scintillometer-derived fluxes to z', will introduce some uncertainty into the results. In the absence of an accepted method to determine z' in the present environment, taking an average value from a number of approaches is the preferred procedure. The final z' values for the canyon SLS and sonic anemometer are 3.4 and 4.4 m, respectively and 4.3 m for the sensors above the roofs. The latter were located about 3.5 m above the local roof surface. If the assumption was made that the roof surface was completely homogeneous (with no roughness elements) an effective measurement height close to the roof surface would be assumed. Given the nature of the probability density function contours, the parameters measured by the SLS are weighted more towards the middle of the path, which stresses contributions from the roof. Contributions from the streets, courtyards and convection off the vertical walls on the other hand will lower the effective measurement height somewhat to below the local roof height. Hence a value that corresponds to about the mean building height for the area seems to be a reasonable estimate.

4 Results

Close to the urban surface the flow is highly directional and inhomogeneous with wakes just above and behind buildings and other structures and preferential flow directions induced by the geometry and arrangement of canyons. Several studies have shown that turbulence characteristics in the RSL do not necessarily obey MOS, which is the preferred framework for analysis and presentation of turbulence statistics in the homogeneous surface layer. The same applies for the dissipation of TKE and

heat and the temperature structure parameter whose non-dimensional forms (Eqs. (3), (7) and (6)) are needed to calculate the sensible heat and momentum fluxes using scintillometery (see Eqs. (13)–(16) for some commonly used surface-layer forms). The following sections investigate some of the turbulence statistics needed for, and assumptions underlying, the application of scintillometery in the urban RSL. Where possible the present results are compared to data from other urban studies and the homogeneous surface layer.

4.1 Spectral shapes and calculation of dissipation values

Dissipation values can be determined from the spectral density estimates in the inertial subrange of the respective velocity and temperature spectra (e.g. Kaimal and Finnigan 1994; Roth 1993 for urban applications). An inertial subrange exists if the following three conditions apply. First, spectra presented in log–log coordinates and using non-dimensional frequency $f\ (= nz'/U)$ are characterized by a constant $-2/3$ slope in the inertial subrange. The turbulence in this range is assumed to be isotropic (locally in wavenumber space). Second, there is a 4/3 ratio between the spectral densities of the transverse (v and w) and streamwise (u) velocity components as a consequence of local isotropy. Third, cospectral levels vanish in the inertial subrange. A correct estimation of dissipation rates is only possible in an undisturbed inertial subrange where local isotropy exists and Taylor's hypothesis is applicable.

The existence of local isotropy was assessed by evaluating the ratio of spectral densities and the high-frequency slope of the spectra. The ratio between the spectral densities of the w and u components in the frequency range where the dissipation values were determined is lower than the theoretical homogeneous surface layer ratio of 4/3 (Table 3). This is the case for the present as well as previous (sub)urban studies, irrespective of the height within the RSL. No dependence on wind speed and direction or stability could be seen in the present data. Isotropy is generally also violated within vegetation canopies where ratios have been found to vary between 0.94 and 1.7 (Kaimal and Finnigan 1994), and lower than predicted ratios are also found in less rough environments too. Mestayer (1982), for example, concludes that, as a general rule, local isotropy and the 4/3 ratio are not attained for measurements within the homogeneous surface-layer inertial subrange. High-frequency X-wire anemometer measurements reviewed by Mestayer show ratios of about 1.1 in the inertial subrange and the 4/3 ratio is not attained until $f > 20$, i.e. frequencies close to the dissipation range of spectra. A possible explanation for spectrum ratio convergence to a lower value (in fact 1.0 at the low frequency end of the inertial subrange (Biltoft 2001) has been proposed by Henjes (1998). She suggests that, for the Taylor transform to be applicable, the averaging time used for the evaluation of the spectra should not exceed the EC decay time, which is usually much less and on the order of seconds. This might be much shorter than current practice.

For Taylor's hypothesis to apply, it is necessary that the turbulence is stationary and homogeneous in the along-wind direction, conditions that are rarely fulfilled in the urban environment, especially close to the urban canopy. Strong vertical wind shear, for example, will generally distort the eddies. Willis and Deardorff (1976) suggest that Taylor's hypothesis becomes inapplicable if turbulent intensities exceed 0.5. The corresponding values for the present observations are 0.5 and 0.65 for the rooftop and canyon-top locations, respectively.

Table 3 Summary of inertial subrange statistics for (sub)urban studies

Study	z/z_H	S_w/S_u	Slope	f	n (s^{-1})	Comments
Rotach (1991)	1.55	0.8	$> -2/3$	3	$\sim 0.6^a$	
	1.27	0.8, 1.1	$> -2/3$	3		Urban (slope for u, v, and w)
	0.91	0.6	$> -2/3$	3		
	0.71	0.75, 1.1	$> -2/3$	3.5, 11		
Roth and Oke (1993)	2.62	1.1–1.2	$-2/3$	2.5–5	$\sim 0.3 - 0.6^a$	Suburban (slope for u, v, and w)
Christen et al. (2004)	2.17	1.14	$> -2/3$	$\sim 0.9 - 9^a$	0.1 – 1	
	1.23	1.03	$> -2/3$	$\sim 0.5 - 5^a$	0.1 – 1	Urban (slope for u)
	1.01	1.15	$> -2/3$	$\sim 0.5 - 5^a$	0.1 – 1	
	0.77	1.05	$> -2/3$	$\sim 0.6 - 6^a$	0.1 – 1	
Present study	1.32	1.11 (0.8–1.4)	–2/3	3 – 6	$\sim 1.1 - 2.3^a$	Urban (slope for w)
	1.01	1.14 (0.7–1.5)	–2/3	4 – 10	$\sim 0.8 - 2.1^a$	

S—spectral energy density, u—longitudinal velocity, w—vertical velocity, f— non-dimensional frequency, n—natural frequency, z—sensor height, z_H—average height of buildings
[a] Based on estimated effective measuring height and average wind speed (where available)

The present w and T spectra show well-defined $-2/3$ slopes within the inertial subrange at both locations and for various stability conditions (Fig. 3). Other urban data, for which simultaneous values for the spectral ratio and the slope are available, show slower high-frequency roll-off compared to the theoretical prediction of $-2/3$ (Table 3). The slope of the velocity spectra are affected by the extra physical processes that operate in the urban RSL. The conversion of kinetic energy of the mean flow to turbulent energy by the wake production mechanism produces eddies with a range of scales that is determined by the dimensions of the roughness elements and depends on the nature of the surface morphology; a range of time and length scales may be associated with these processes. The result will be higher spectral levels (i.e. smaller roll-off) within the inertial subrange if small production rates still exist at these frequencies. This has, for example, been observed in plant canopies. Kaimal and Finnigan (1994) note that here the aerodynamic drag is most efficient in extracting energy from the u component, which ensures that the v and w fluctuations will be boosted at the expense of u fluctuations. A sample of present and past (sub)urban observations, however, shows all components to be equally affected (Fig. 3; Table 3). The present data experience no or little contamination of the inertial subrange where small-scale turbulence production rates are insignificant compared to the size of the energy input at larger scales. Any effect on the calculation of the dissipation values (Sect. 4.2) and the non-dimensional dissipation functions (Sect. 4.3) should therefore also be small.

4.2 Basic scintillometer statistics and comparison of scintillometer and eddy-correlation dissipation values

The basic variables measured by the SLS are l_0 and C_n^2 from which the turbulent fluxes are derived. Figure 4 shows the variation of these two variables together with ε and U. Generally l_0 is inversely related to U, reaching values of up to 9 mm at both levels.

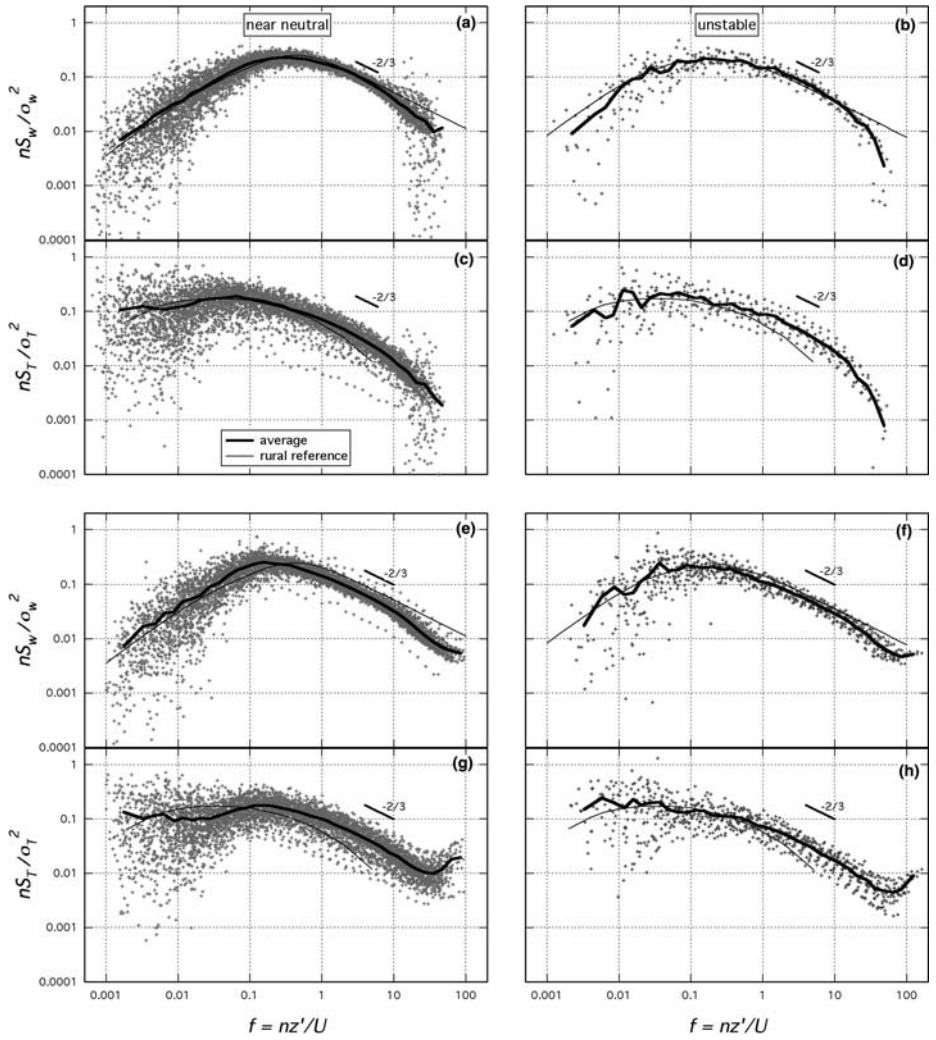

Fig. 3 Normalized spectra for near neutral ($-0.1 < z'/L_v < 0$) (left column) and unstable ($z'/L_v < -1$) (right column) conditions of w and T measured above (**a**) – (**d**) rooftop ($z/z_H = 1.32$) and (**e**)–(**h**) canyon ($z/z_H = 1.01$) plotted against non-dimensional frequency on a log-log plot. The short dark solid lines indicate the $-2/3$ slope and range over which dissipation values have been calculated (see text for more details). The thick solid lines are averages of the individual spectra (crosses); the thin solid lines are a model based on rural reference data evaluated at $z'/L_v = -0.005$ in (**a**) and (**e**) and $z'/L_v = -1$, in (**b**) and (**f**) (Panofsky et al. 1977; Højstrup 1981) and for slightly unstable conditions in (**c**), (**d**), (**g**) and (**h**) (Anderson and Verma 1985)

High wind speeds increase the dissipation rate of TKE, where typical ε values are $< 0.05\,\mathrm{m^2\,s^{-3}}$ above the rooftops and larger values of up to $0.11\,\mathrm{m^2\,s^{-3}}$ are possible above the canyon, highlighting the influence of the mechanically driven turbulence on TKE production and dissipation. Typically C_n^2 values have a maximum around noon, when Q_H is highest, with higher values observed above the rooftops. Although these periods are often associated with increasing wind speeds, the urban area is still able

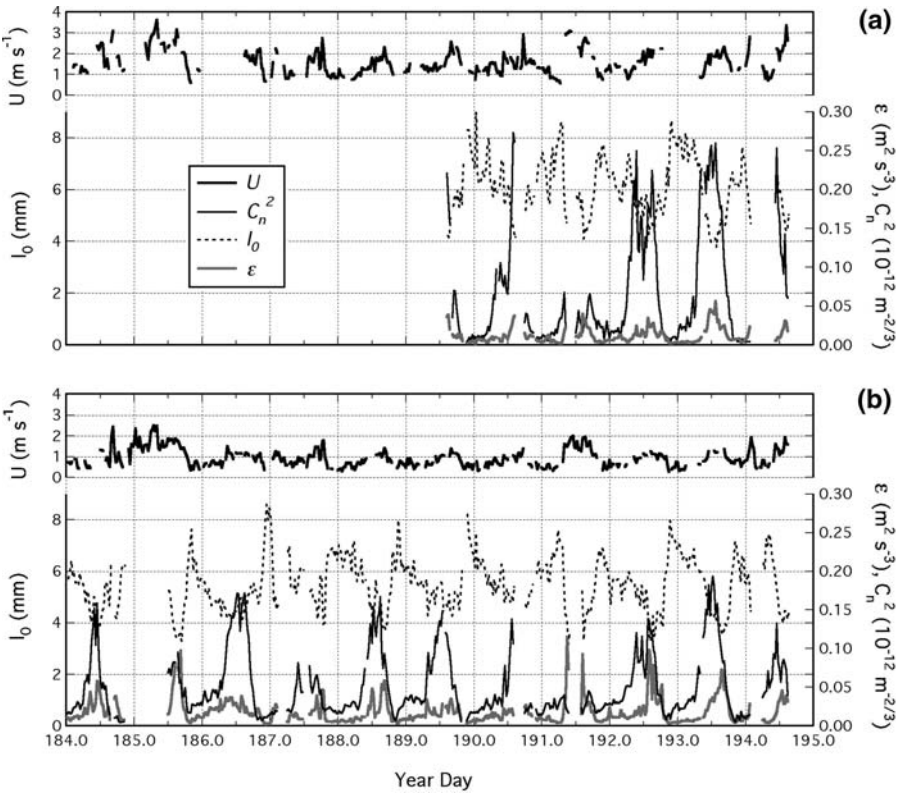

Fig. 4 Time series of 30-min averages of mean wind speed (U), inner length scale (l_0), dissipation (ε), and refractive index structure parameter structure (C_n^2) for July 3–13, 2002, measured above (**a**) rooftops ($z/z_H = 1.32$) and (**b**) canyon ($z/z_H = 1.01$)

to maintain large vertical temperature gradients and hence high sensible heat fluxes during these times.

EC dissipation rates can be estimated from all three velocity components, and Fig. 5a and c compare the ε values derived from the u and w components. Scatter is small at both measurement levels but the rooftop values based on the u spectra are systematically larger compared to those obtained from the w spectra. The same trend is seen above the canyon for small values. Dissipation rates based on v spectra were usually slightly smaller than those based on the w component (not shown). Differences in ε values may be due to different spectral densities in the inertial subrange, i.e. the 4/3 ratio between the transverse and streamwise velocity components is not attained, indicating an absence of local isotropy as already noted above (Table 3). This is despite the fact that the u spectra exhibit a well-defined $-2/3$ slope in the inertial subrange (not shown). Dissipation values based on the w spectra were chosen for the present study, mainly because they lay between those from the u and v spectra. In addition the spectral energy distribution of the vertical wind component is shifted towards higher frequencies and smaller eddies should reach local equilibrium faster and result in less distortion of the spectral shape.

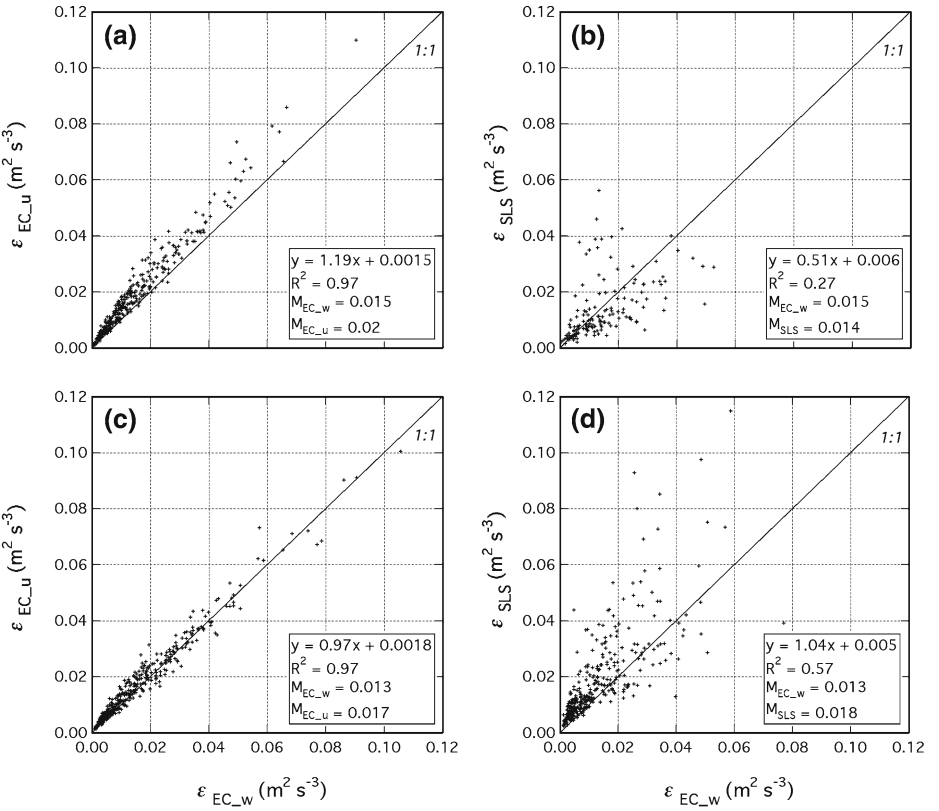

Fig. 5 Scatter plot of 30-min averages of dissipation values obtained from EC spectra of vertical (w) and longitudinal (u) velocity and from scintillometer (SLS) above (**a**)–(**b**) rooftops and (**c**)–(**d**) canyon. R^2—correlation coefficient; M_{EC_w}—mean of EC values based on w spectra, M_{EC_u}—mean of EC values based on u spectra, M_{SLS}—mean of SLS values. (**b**) and (**d**) only include data from periods with concurrent EC and SLS measurements

To estimate the influence of the location of the frequency range within which ε is calculated the present results from above the rooftops have been compared to re-calculated values for the range $f = 1.3$–4 where slopes are slightly less than the inertial subrange prediction (Fig. 3a–d). Differences were small with average values 4% (1%) lower for ε (N^*) and individual ε and N^* values differed by less than $\pm 20\%$. This is a further indication that the calculation of the dissipation values is relatively insensitive to the shape of the spectral slope.

Present and previous urban work has illustrated the various issues associated with the applicability of MOS close to the urban canopy. Comparing ε values from the SLS and EC systems (Eqs. (1) and (20)) provides the only direct comparison of the two different approaches that is independent of MOS scaling. ε derived from the SLS is generally smaller compared to ε derived from EC above the rooftops but the reverse is true over the canyon (Fig. 5b, d). Even for the homogeneous surface layer Hartogenesis et al. (2002) point to the possibility of a systematic underestimation at high values of ε by the SLS arising from the particular value used for the beam displacement distance in the SLS software. Additional uncertainty at the canyon-top

level arises because of the different effective heights of the two sensors (Table 1). Since the height variation of ε is unknown within the canyon a correction was not attempted. Given that the height difference is small and turbulence properties are well mixed in the upper part of a canyon this effect is likely to be small. The large scatter in the present data, however, cannot only be attributed to the completely different techniques used. Given the spatial inhomogeneity of the RSL, in particular close to the surface, the different source areas that are associated with line average and point statistics will have an influence on the comparison. For example, the TKE dissipation associated with the canyon walls will contribute to the SLS observations but be missed by the EC sensor whose source area is smaller.

4.3 Calculation of urban forms of the **MOS** equations using eddy correlation data

The non-dimensional dissipation functions for TKE (ϕ_ε), temperature variance (ϕ_N) and structure parameter for temperature (ϕ_{CT}) based on the EC observations for the rooftop and canyon locations are presented in Figures 6 and 7. The scatter in the data is large, especially above the canyon. Functions have been fitted through median averages determined at equally spaced intervals along the log $-z'/L_v$ axis (local scaling is used, i.e. all variables are measured locally). The present ϕ_ε fit for the canyon-top location is, as expected, close to that from a longer dataset consisting of hourly averages presented by Christen et al. (2004) with the exception of the near-neutral range where, however, only few data points are available (Fig. 7a). At both heights the ϕ_ε empirical fits deviate from previous urban observations. The prominent dip observed between $z'/L_v = -0.5$ and -0.1 in the urban results based on two suburban sites at $z/z_H > 2.5$ (Kanda et al. 2002) is less pronounced in the present data above the rooftops (Fig. 6a) and absent over the canyon (Fig. 7a). Compared to results from the homogeneous surface layer agreement at the rooftop location is good at neutral and near-neutral stability but the present results become increasingly larger as instability increases (Fig. 6a). The canyon-top data are generally smaller (larger) at near-neutral (moderate) instability (Fig. 7a).

It is not surprising that the canyon-top ϕ_ε data show the strongest deviations from the reference. The interface where the exchange of the canyon air and the above-canyon flow occurs is dynamically unstable, influenced by wake shedding off the nearby roofs and rooftop structures and as a consequence characterized by the absence of a logarithmic wind profile. The results suggest $\phi_\varepsilon < 1$ near the top of the canyon under neutral and near-neutral conditions (Fig. 7a), implying an absence of equilibrium between production and dissipation of TKE i.e. turbulence is generated more rapidly than it is dissipated locally. Similar results have been observed over suburban surfaces at $2.6 < z/z_H < 3.8$ (Clarke et al. 1982; Roth and Oke 1993; Kanda et al. 2002) at near-neutral and slightly unstable conditions but also close to the surface in the homogeneous rural surface layer (e.g. Oncley et al. 1996; Frenzen and Vogel 2001). In regions of active production of turbulence, transfer along the energy cascade towards the local dissipation scales may become saturated thereby increasing the imbalance between production and dissipation (Frenzen and Vogel 2001). Near the top of the canyon TKE is likely to be transported away to higher or lower, less productive levels and hence will not be available for local dissipation, as shown by Christen et al. (2004) based on an analysis of all components of the TKE balance.

The urban values for ϕ_N increase strongly towards $-z'/L_v = 0.0$ (Figs. 6b, 7b). This is expected given the results from previous urban experiments, which show that T_*

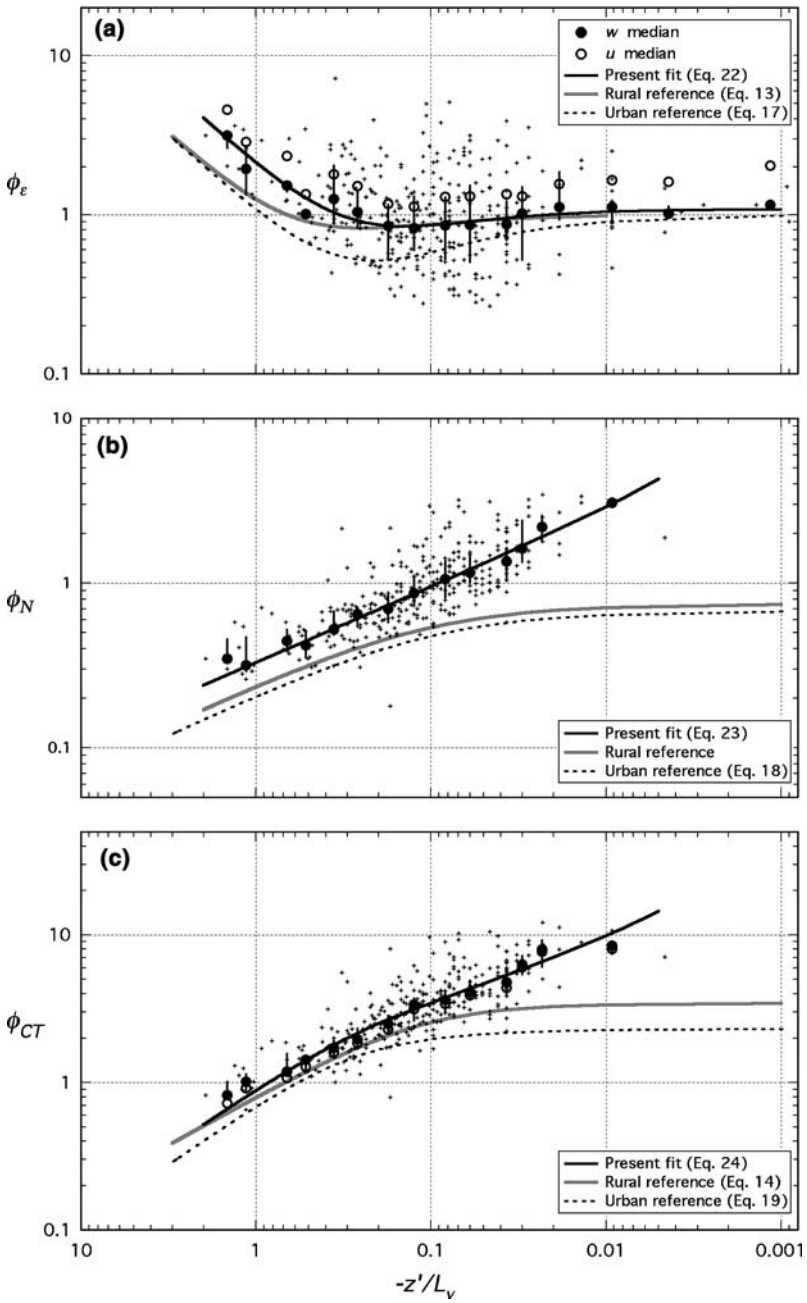

Fig. 6 Non-dimensional dissipation functions measured above rooftops ($z/z_H = 1.32$) for (**a**) TKE, (**b**) temperature variance and (**c**) structure parameter for temperature plotted against non-dimensional stability parameter. Filled (open) circles are median values of calculations using w (u) spectra; error bars indicate the range between the 25% and 75 % quartiles. Black solid line is the fit through w median values, dashed line is the fit to urban data (Kanda et al., 2002), and gray solid lines are a rural reference given in (**b**) as $\phi_N(\zeta) = 0.74\,(1 - 9\zeta)^{-1/2}$ (Wyngaard and Coté 1971)

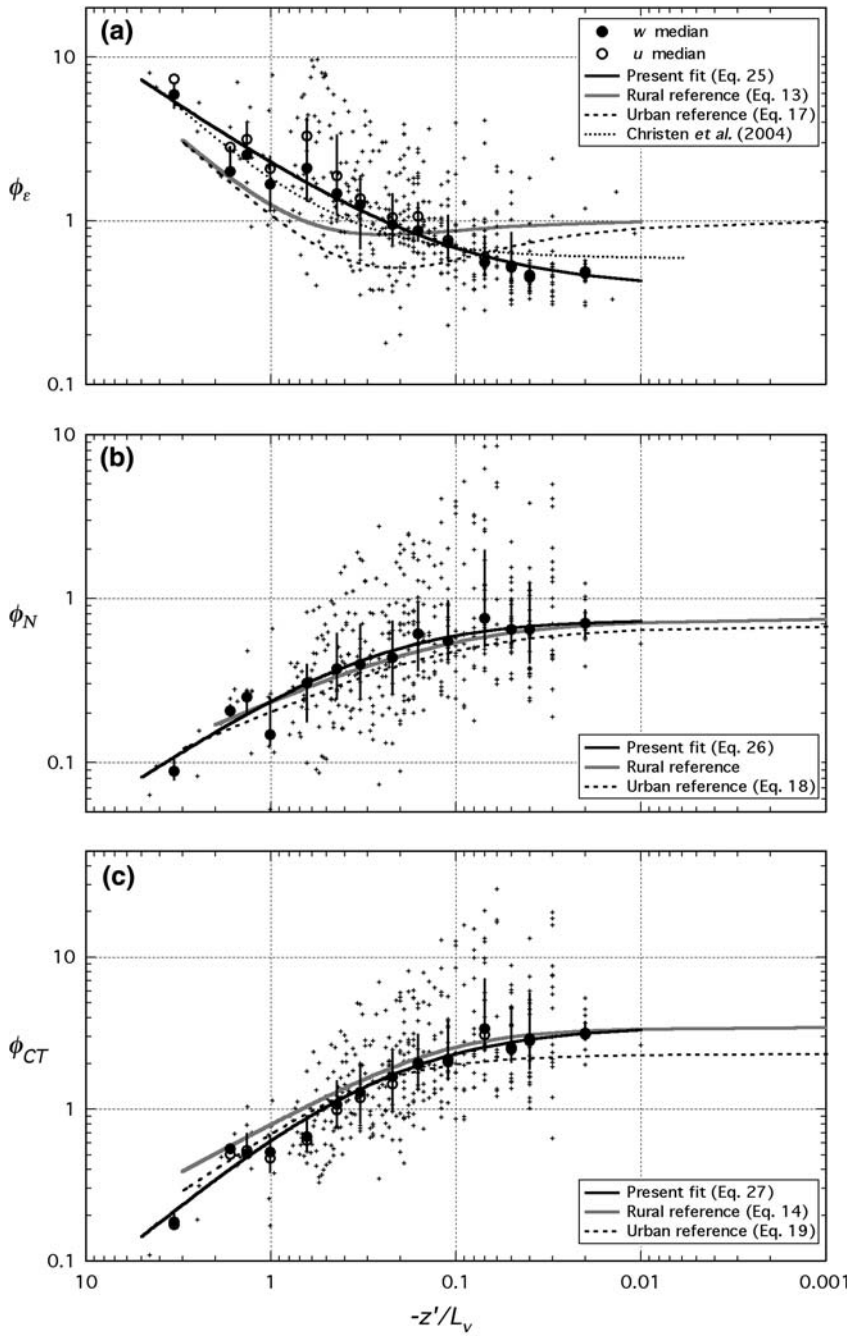

Fig. 7 Same as Fig. 5 but above canyon ($z/z_H = 1.01$). Dotted line is the fit to urban data from the present experiment but for a longer time period (Christen et al. 2004)

tends towards zero when conditions are close to neutral (Roth 2000). However, this feature was not captured by past ϕ_N variations for urban environments (ϕ_N values are 0.7 at $z'/L_v = 0$). Thus the revised forms of the equations for ϕ_N at the present site provide an improved approximation. At larger instabilities the present urban form of the equation is systematically larger compared to the rural and urban references above the rooftops but similar above the canyon.

The resulting form of ϕ_{CT} (Eq. (6)) for the rooftop values is larger, in particular towards neutral conditions (Fig. 6c) because the higher values of ϕ_N are not cancelled out by slightly lower ϕ_ε values. ϕ_{CT} values for the canyon top are similar to those of the reference equations for near-neutral and unstable stratification (Fig. 7c).

The scatter observed in the data is in part a consequence of the inhomogeneity of the flow and hence fetch characteristics. To investigate the potential dependence of turbulence characteristics on flow direction in respect to the canyon orientation the data were divided into eight groups, each representing a 45 degree wind direction sector. The majority of the data are from wind directions parallel to the canyon (i.e. 45–90° and 225–270°) and small angles to the canyon (270–315°), respectively. Relatively few data points are available for flow perpendicular to the canyon (Fig. 2). No trends could be observed between individual sectors and any systematic differences were masked by the large degree of scatter shown by the data. The results presented above are therefore based on all data points from all sectors.

The following equations are empirical fits to the data shown in Figures 6 and 7 and will be used in the calculation of the SLS statistics in Section 4.4 (the respective ϕ_{CT} equations follow from Eq. (6)):
Rooftop ($z/z_H = 1.32$):

$$\phi_\varepsilon(\zeta) = (0.93 - 5.4\zeta)^{-1.1} - 2\zeta, \qquad (-2 < \zeta \leq -0.001) \tag{22}$$

$$\phi_N(\zeta) = 1.42\,(-0.03 - 24\zeta)^{-0.46}, \qquad (-2 \leq \zeta \leq -0.005) \tag{23}$$

$$\phi_{CT}(\zeta) = 3.44\left[1.42(-0.03 - 24\zeta)^{-0.46}\right] \times \left[(0.93 - 5.4\zeta)^{-1.1} - 2\zeta\right]^{-1/3}. \qquad (-2 < \zeta \leq -0.005) \tag{24}$$

Canyon-top ($z/z_H = 1.01$):

$$\phi_\varepsilon(\zeta) = 0.38 + 1.9\,|\zeta|^{0.8}, \qquad (-5 < \zeta \leq -0.01) \tag{25}$$

$$\phi_N(\zeta) = 0.8\,(1.1 - 4\zeta)^{-0.75}, \qquad (-5 < \zeta \leq -0.01) \tag{26}$$

$$\phi_{CT}(\zeta) = 3.44\left[0.8\,(1.1 - 4\zeta)^{-0.75}\right]\left[0.38 + 1.9\,|\zeta|^{0.8}\right]^{-1/3}. \qquad (-5 < \zeta \leq -0.01) \tag{27}$$

4.4 Applying the new urban forms of **MOS** equations to the scintillometer heat and momentum fluxes

One of the objectives of the present study is to comment on the use of the SLS to measure the turbulent fluxes of sensible heat and momentum (i.e. friction velocity) in the urban RSL. The comparison of Q_H and u_* as determined from optical scintillation with those measured directly by EC for the two locations is shown in Fig. 8. Considering the different methods and assumptions involved, the comparison is very good for Q_H above the rooftops (Fig. 8a); SLS values are slightly higher in the case of very low and high fluxes, respectively. One limitation of scintillometery is that there is no means of distinguishing between a positive and a negative heat flux. However, given that the EC

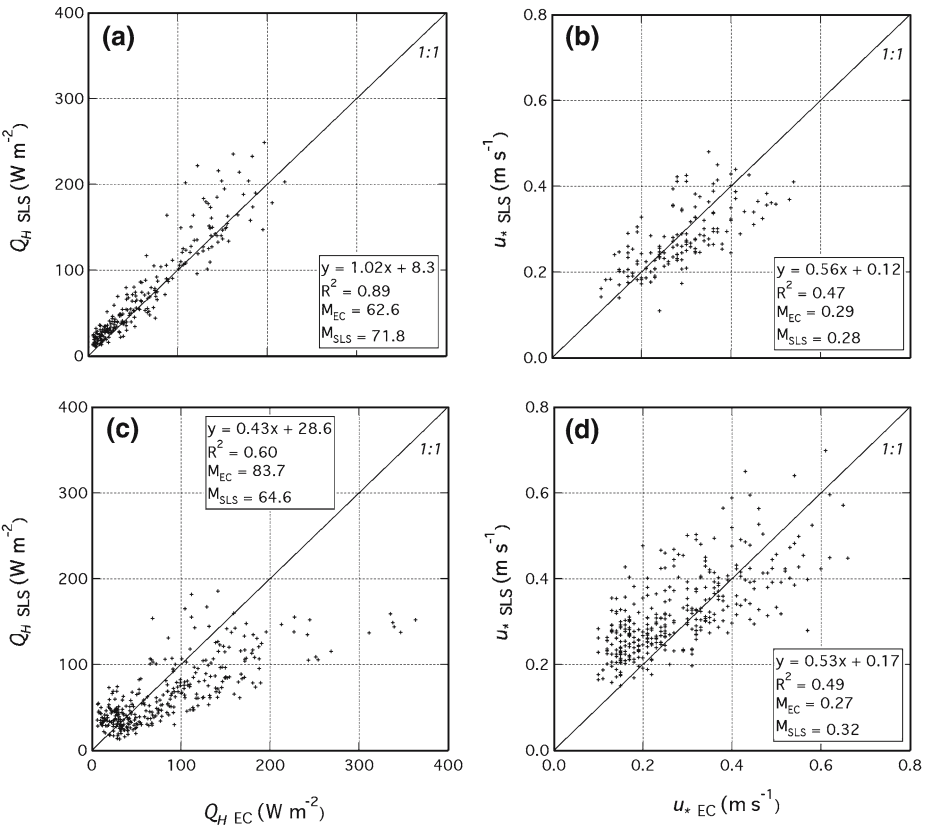

Fig. 8 Scatter plot of 30-min averages of sensible heat flux (Q_H) and friction velocity (u_*) obtained from EC and scintillometer (SLS) above (**a**)–(**b**) rooftops and (**c**)–(**d**) canyon. R^2 — correlation coefficient; M_{EC} – mean of EC values, M_{SLS} —mean of SLS values

heat fluxes remain positive throughout the night (which is usual for an urban surface) this is unlikely to account for the differences observed at low values. Replacing the homogeneous surface-layer MOS functions (Eqs. (13) and (14)) in the SLS software with the new urban forms developed above results in a slightly improved correlation with the EC fluxes and a reduction of the mean error from 22.6 to 9.2 W m^{-2} (not shown). The agreement is similar to that observed during detailed comparisons over rural surfaces by Thiermann and Grassl (1992) for $15 < Q_H < 160$ W m^{-2}, Weiss et al. (2001) and Weiss (2002) for $20 < Q_H < 140$ W m^{-2} and slightly worse compared to the limited urban dataset by Kanda et al. (2002) for $-20 < Q_H < 180$ W m^{-2}.

Above the canyon correlation between the two methods to measure Q_H is reduced. SLS values are again larger compared to the EC results if magnitudes are low but the reverse is true for large fluxes (Fig. 8c). This is similar to the urban results of Lagouarde et al. (2006) who also reported higher Q_H values from the LAS compared to the EC during nighttime when fluxes are small. Small fluxes are associated with near-neutral conditions occurring at night. It is possible that the differences are due to the increased spatial sampling along the optical scintillometer path, since scintillometers are capable of measuring sensible heat flux contributions from e.g. the canyon

walls that the EC sensor would miss. This is explored more fully in Salmond et al. (2003).

Agreement for u_* is less at both levels although the mean error (especially above the roofs) is relatively small (Fig. 8b, d). The SLS values tend to be larger (smaller) compared to the EC observations for small (large) values, where small (large) u_* values are generally associated with very unstable (near-neutral) conditions. The lack of correlation is largely a product of the high degree of scatter associated with the calculation of ϕ_ε due to the reasons mentioned earlier. The lack of agreement between ε determined by the two methods (Fig. 5b, d) is responsible for a similar lack of agreement for u_* since the latter is directly related to ε and hence ϕ_ε (Eq. (3)). Q_H is more robust because it is calculated from ϕ_{CT} and dependence on ϕ_ε is less (Eq. (6)).

A number of studies have commented on the difficulties of calculating u_* using scintillometery. De Bruin et al. (2002) and Hartogensis et al. (2002) also reported a small systematic underestimation (overestimation) for high (low) u_* values, which they were able to minimize by using a model to correct for random noise and inactive turbulence and by adjusting the beam displacement distance of the SLS. Lack of isotropy may also affect the quality of the ε estimates and hence fluxes. This has been investigated by Weiss (2002). Using measurements when spectral ratios were $\neq 4/3$ did, however, not affect Q_H and only resulted in a small underestimation by the SLS for small u_* under near-neutral conditions.

5 Summary and conclusions

The present study investigates the operational performance of a displaced-beam small-aperture SLS in the urban roughness sublayer (RSL). Turbulence characteristics and fluxes were measured using a SLS and EC sensor co-located with the mid-point of the optical SLS path above rooftops and across a canyon, respectively, which are the two dominant components of the urban surface. The main results are:

(1) Application of scintillometery requires accurate knowledge of the effective measurement height, z'. Because of the difficulty of defining the "actual surface" that contributes to a flux measurement, z' has been estimated as the average value from a range of available morphometric approaches. Variability between the values from the various equations is relatively small at the rooftop location ($\pm 15\%$) but larger above the canyon; z' values are similar but not the same at the two locations. This result seems reasonable because different surface facets at different heights are sampled by a sensor located above a canyon or rooftops, respectively.
(2) The first values of l_0 and C_n^2 from a city are presented. The data show the influence of mechanically driven turbulence on dissipation and the refractive index fluctuations. l_0 is inversely related to mean wind speed and C_n^2 has a maximum around noon, which is a period of high Q_H but also of higher wind speeds.
(3) Comparing ε values from the SLS and the EC system provides the only way for a direct comparison of the two different approaches that is independent of MOS scaling. Dissipation values obtained from the u and w velocity components correlate very well with each other, although a small systematic difference can be observed at the rooftop level where ε derived from the u spectrum is slightly larger. Comparison of ε from the SLS and EC sensors is marked by much scatter,

and is probably due to the different assumptions underlying the derivation of the values and the spatial heterogeneity of the surface, i.e. source areas "seen" by the SLS and EC sensor differ. It is possible that the generally larger canyon ε values from the SLS are due to its ability to sense turbulence processes associated with the canyon walls that may not be sampled by the single-point EC sensor.

(4) The non-dimensional dissipation functions are calculated from dissipation values determined within the inertial subrange of the corresponding w and T spectra. A correct estimation of dissipation rates is only possible if local isotropy exists and Taylor's hypothesis is applicable. The ratio between the spectral densities of the w and u velocity components is less than 4/3 required for local isotropy, a result that is also true for other (sub)urban studies. On the other hand the present results reveal the predicted and required (for local isotropy) $-2/3$ slope at the high frequency end of the w and T spectra. Estimating ε within a frequency band outside the $-2/3$ slope had a negligible influence on the values. Based on this evidence it appears that the existence of a $-2/3$ slope is a relatively insensitive indication of local isotropy and its absence may not affect the calculation of the fluxes.

(5) Despite the fact that MOS does not apply in the RSL it is necessary to calculate urban forms of the non-dimensional dissipation rates for the potential application of scintillometery in the urban environment. Similar to other turbulence statistics obtained at the present site the scatter in the data is large. Functions fitted through median averages are similar (higher) to the homogeneous surface layer for ϕ_ε (ϕ_N and ϕ_{CT}) above the rooftops. The present results indicate an absence of equilibrium between production and dissipation of TKE near the canyon top, which is a region of active production of turbulence. ϕ_N and ϕ_{CT} show surprisingly good agreement with homogeneous surface-layer data at this level. The prominent dip observed at near-neutral and slightly unstable conditions in other urban data obtained near the top of the RSL is less pronounced (rooftop) or absent (canyon) in the present observations. It should be noted that calculation of the non-dimensional dissipation functions is almost independent of the choice of z'. For example increasing z' will increase ϕ_ε according to Equation (3) but will also increase the absolute value of $-z'/L_v$ against which ϕ_ε is plotted.

(6) Q_H values from the two methods agree well with each other above the rooftops but agreement is less above the canyon. For small (large) values, which usually occur at night (in the middle of the day), SLS fluxes are generally higher (smaller) than those measured by the EC system. This is likely to be the result of the improved spatial sampling by the SLS. We hypothesize that at night the SLS is able to measure the positive contributions from the canyon walls that will be missed by the EC system. Similarly, during daytime Q_H from the SLS may be smaller because the line-averaged values include the relatively low fluxes from the shaded walls. Correlation statistics are worse for u_* with the SLS observations being larger (smaller) at small (large) values. A number of studies have commented on the difficulties of calculating u_* using scintillometery; this problem is not limited to the application of scintillometers in urban areas and needs further exploration.

The present observations have been conducted in a region of extreme spatial heterogeneity in surface structure and variability of turbulence characteristics and fluxes.

The good agreement between Q_H measured by the SLS and EC approaches above the rooftops is therefore quite surprising and the analysis suggests that scintillometery may be an appropriate tool for the measurement of Q_H at this level. However, the procedure requires careful determination of z_d and the use of urban forms of the MOS equations. If universal urban MOS functions could be derived scintillometery would become self-sufficient for operational applications in the RSL. At this point it is not possible to determine if the lesser agreement above the canyon is due to inadequate spatial sampling by the EC sensors or some other reason.

Because of the difficulties associated with the determination of ϕ_ε in the RSL from single-point EC observations, the suitability of the scintillometers for estimating momentum fluxes remains inconclusive. The present measurements are unable to explain the large scatter and systematic ϕ_ε differences observed, which reinforces the need for the continued development and refinement of urban forms of the equations and a more thorough assessment of the influence the absence of an inertial subrange might have on the determination of ε. This problem is less for Q_H, which is estimated from ϕ_{CT} calculated from the ratio of ϕ_N and $\phi_\varepsilon^{1/3}$, and hence potential errors in C_n^2 and l_0 tend to cancel out in the SLS procedure to determine Q_H (De Bruin et al. 2002).

A full analysis of the role different source areas have in causing the variability seen between the two approaches would require multiple EC sensors along the same scintillometer path. Nevertheless the interpretation of the results above illustrates the possibility of improved spatial representativeness of scintillometer data. Small differences in the heat storage capacity and thermal admittance of different building materials may result in marked variations in the heat fluxes emitted from different surfaces, especially at night. In this scenario we might expect the scintillometer to provide a more representative measurement of the sensible heat fluxes from the urban area as a whole.

Acknowledgements Special thanks go to Andreas Christen (Technological University of Berlin) for his support with data acquisition and data dissemination and Tim Oke (University of British Columbia) for his help and support during the field experiment and throughout the preparation of this manuscript. This experiment was possible thanks to the generosity of Roland Vogt (University of Basel) and Manabu Kanda (Tokyo Institute of Technology) who loaned the scintillometers. All members of the BUBBLE staff of University Basel and ETH (Zürich) are thanked for their outstanding support of this project. Funding for this research has been provided by the National University of Singapore (R–109–000–037–112). The Canadian Foundation for Climate and Atmospheric Science (CFCAS) and the Natural Science and Engineering Research Council of Canada (NSERC) provided further financial support.

References

Anderson DE, Verma SB (1985) Turbulence spectra of CO_2, water vapour, temperature and wind velocity fluctuations over a crop surface. Boundary-Layer Meteorol 33:1–14

Andreas EL, Fairall CW, Persson POG, Guest PS (2003) Probability distributions for the inner scale and the refractive index structure parameter and their implications for flux averaging. J Appl Meteorol 42:1316–1329

Biltoft CA (2001) Some thoughts on local isotropy and the 4/3 lateral to longitudinal velocity spectrum ratio. Boundary-Layer Meteorol 100:393–404

Bottema M (1995) Aerodynamic roughness parameters for homogeneous building groups – Part 2: Results document SUB–MESO 23. Ecole Central de Nantes, France, 80 pp

Christen A, Vogt R (2004) Energy and radiation balance of a central European city. Int J Climatol 24:1395–1421

Christen A, Rotach MW, Vogt R (2004) Experimental determination of the urban kinetic energy budget within and above an urban canyon. In: Proceedings, fifth symposium on the urban environment. Vancouver, Canada, August 23–26, 2004, American Meteorological Society, 45 Beacon St., Boston, MA, (CD–ROM)

Clarke JF, Ching JKS, Godowitch JM (1982) An experimental study of turbulence in an urban environment. Tech. Rep. U.S. E.P.A., Research Triangle Park, N.C. NMS PB 226085, 155 pp

Corrsin S (1951) On the spectrum of isotropic temperature fluctuations in isotropic turbulence. J Appl Phys 22:469–473

De Bruin HAR, Meijninger WML, Smedman AS, Magnusson M (2002) Displaced-beam small aperture scintillometer test. Part 1: The Wintex data set. Boundary-Layer Meteorol 105:129–148

Feigenwinter C, Vogt R, Parlow E (1999) Vertical structure of selected turbulence characteristics above an urban canyon. Theor Appl Climatol 62:51–63

Frenzen P, Vogel CA (1992) The turbulent kinetic energy budget in the atmospheric surface layer. A review and experimental re-examination in the field. Boundary-Layer Meteorol 60:49–76

Frenzen P, Vogel CA (2001) Further studies on atmospheric turbulence in layers near the surface: scaling the TKE budget above the roughness sublayer. Boundary-Layer Meteorol 99:173–206

Green AE, McAneney KJ, Astill MS (1994) Surface-layer scintillation measurements of daytime sensible heat and momentum fluxes. Boundary-Layer Meteorol 68:357–373

Grimmond CSB, Oke TR (1999) Aerodynamic properties of urban areas derived from analysis of surface form. J Appl Meteorol 38:1262–1292

Hartogensis OK, De Bruin HAR, van de Weil JH (2002) Displaced-beam small aperture scintillometer test. Part II: CASES–99 Stable boundary-layer experiment. Boundary-Layer Meteorol 105:149–176

Henjes K (1998) Justification of the inertial dissipation techniques in anisotropic mean flow. Boundary-Layer Meteorol 88:161–180

Hill RW (1997) Algorithms for obtaining atmospheric surface-layer fluxes from scintillation measurements. J Atmos Oceanic Tech 14:456–467

Hill RW, Ochs GR, Wilson JJ (1992) Measuring surface-layer fluxes of heat and momentum using optical scintillation. Boundary-Layer Meteorol 58:391–408

Højstrup J (1981) A simple model for the adjustment of velocity spectra in unstable conditions downstream of an abrupt change in roughness and heat flux. Boundary-Layer Meteorol 21:341–356

Irvine MR, Lagouarde J-P, Bonnefond J-M, Grimmond S, Oke TR (2002) Sensible heat flux estimated over the city of Marseille, using a LAS Scintillometer. In: Proceedings, fourth symposium on the urban environment, Norfolk, Virginia, May 20–24, 2002, American Meteorological Society, 45 Beacon St., Boston, pp 215–216

Kaimal JC, Wyngaard JC, Izumi Y, Coté OR (1972) Spectral characteristics of surface-layer turbulence. Quart J Roy Meteorol Soc 98:563–589

Kaimal JC, Finnigan JJ (1994) Atmospheric boundary layer flows – their structure and measurement. Oxford University Press, New York, 289 pp

Kanda M, Takayanagi Y, Yokoyama H, Moriwaki R (1997) Field observation of the heat balance in an urban area. J Japan Soc Hydrol Water Resour 10:329–336 (in Japanese)

Kanda M, Moriwaki R, Roth M, Oke TR (2002) Area-averaged sensible heat flux and a new method to determine zero-plane displacement length over an urban surface using scintillometery. Boundary-Layer Meteorol 105:177–193

Kohsiek W (1982) Measuring C_T^2, C_Q^2 and C_{TQ} in the unstable surface layer, and relations to the vertical fluxes of heat and moisture. Boundary-Layer Meteorol 24:89–107

Lagouarde J-P, Irvine M, Bonnefond J-M, Grimmond CSB, Long N, Oke TR, Salmond JA, Offerle B (2006) Monitoring the sensible heat flux over urban areas using large aperture scintillometery: case study of Marseille city during the ESCOMPTE experiment. Boundary-Layer Meteorol 118:xx–xx

Liu H, Peters G, Foken T (2001) New equations for sonic temperature variance and buoyancy heat flux with an omnidirectional sonic anemometer. Boundary-Layer Meteorol 100:459–468

MacDonald RW, Griffiths RF, Hall DJ (1998) An improved method for estimation of surface roughness of obstacle arrays. Atmos Environ 32:1857–1864

Mestayer P (1982) Local isotropy and anisotropy in a high-Reynolds-number turbulent boundary layer. J Fluid Mech 125:475–503

Mestayer PG, Durand P, Augustin P, Bastin S, Bonnefond J-M, Bénech B, Campistron B, Coppalle A, Delbarre H, Dousset B, Drobinski P, Druilhet A, Fréjafon E, Grimmond CSB, Groleau D, Irvine M, Kergomard C, Kermadi S, Lagouarde J-P, Lemonsu A, Lohou F, Long N, Masson V, Moppert C, Noilhan J, Offerle B, Oke TR, Pigeon G, Puygrenier V, Roberts S, Rosant J-M, Said F, Salmond J, Talbaut M, Voogt J (2005) The urban boundary-layer field campaign in Marseille (UBL/CLU–ESCOMPTE): set-up and first results. Boundary-Layer Meteorol 114:315–365

Monin AS, Obukhov AM (1954) Basic laws of turbulent mixing in the ground layer of the atmosphere. Trans Geophys Inst Akad Nauk USSR 151:163–187
Oncley SP, Friehe CA, LaRue JC, Busing JA, Itsweire EC, Change SS (1996) Surface layer fluxes, profiles and turbulence measurements over uniform terrain under near-neutral conditions. J Atmos Sci 53:1029–1044
Panofsky HA, Tennekes H, Lenschow DH, Wyngaard JC (1977) The characteristics of turbulent velocity components in the surface layer under unstable conditions. Boundary-Layer Meteorol 11:355–361
Raupach M (1994) Simplified expressions for vegetation roughness length and zero-plane displacement as functions of canopy height and area index. Boundary-Layer Meteorol 71:211–216
Rotach MW (1991) Turbulence within and above an urban canyon. Zürcher Geographische Schriften, No. 45, ETH Zürich, Switzerland, 245 pp
Rotach MW (1993a) Turbulence close to a rough urban surface Part I: Reynolds stress. Boundary-Layer Meteorol 65:1–28
Rotach MW (1993b) Turbulence close to a rough urban surface Part II: Variances and gradients. Boundary-Layer Meteorol 66:75–92
Rotach MW, Vogt R, Bernhofer C, Batchvarova E, Christen A, Clappier A, Feddersen B, Gryning S-E, Martucci G, Mayer H, Mitev V, Oke TR, Parlow E, Richner H, Roth M, Roulet Y-A, Ruffieux D, Salmond JA, Schatzmann M, Vogt JA (2005) BUBBLE – an urban boundary layer meteorology project. Theor Appl Climatol 81:231–261
Roth M (1993) Turbulent transfer relationships over an urban surface. II: Integral statistics. Quart J Roy Meteorol Soc 119:1105–1120
Roth M (2000) Review of atmospheric turbulence over cities. Quart J Roy Meteorol Soc 126:941–990
Roth M, Oke TR (1993) Turbulent transfer relationships over an urban surface. I: Spectral characteristics. Quart J Roy Meteorol Soc 119:1071–1104
Salmond JA, Roth M, Oke TR, Satyanarayana ANV, Vogt R, Christen A (2003) Comparison of turbulent fluxes from roof top versus street canyon locations using scintillometers and eddy covariance techniques. In: Proceedings, fifth international conference on urban climate, Lodz, Poland, September 1–5, 2003, International Association for Urban Climate, pp 317–320
Schmid HP (1994) Source areas for scalars and scalar fluxes. Boundary-Layer Meteorol 67:293–318
Thiermann V, Grassl H (1992) The measurement of turbulent surface-layer fluxes by use of bichromatic scintillation. Boundary-Layer Meteorol 58:367–389
Vogel CA, Frenzen P (1992) A new study of the TKE budget in the surface layer. Part II: The dissipation function and divergent transport terms. In: Proceedings, tenth symposium on turbulence and diffusion, Portland, Oregon, September 29–October 2, 1992, American Meteorological Society, 45 Beacon St., Boston pp 161–164
Webb EK, Pearman GI, Leuning R (1980) Correction of the flux measurements for density effects due to heat and water vapour transfer. Quart J Roy Meteorol Soc 106:85–100
Weiss AI, Hennes M, Rotach MW (2001) Derivation of refractive index and temperature gradient from optical scintillometery to correct atmospherically induced errors for highly precise geodetic measurements. Surveys Geophys 22:589–596
Weiss AI (2002) Determination of thermal stratification and turbulence of the atmospheric surface layer over various types of terrain by optical scintillometery. Ph.D. Dissertation, No. 14514, ETH Zürich. Switzerland, 152 pp
Willis GE, Deardorff JW (1976) On the use of Taylor's hypothesis for diffusion in the mixed layer. Quart J Roy Meteorol Soc 102:817–822
Wyngaard JC (1973) On surface-layer turbulence. In: Haugen DA (ed) Workshop on micrometeorology, pp 101–149
Wyngaard JC, Coté OR (1971) The budgets of turbulent kinetic energy and temperature variance in the atmospheric surface layer. J Atmos Sci 28:190–201
Wyngaard JC, Coté OR, Izumi Y (1971) Local free convection, similarity and the budgets of shear stress and heat flux. J Atmos Sci 37:271–284